JACS
JOURNAL OF THE AMERICAN CHEMICAL SOCIETY
Article
pubs.acs.org/JACS

Chemistry and Structure of a Host–Guest Relationship: The Power of NMR and X-ray Diffraction in Tandem

Qi-Qiang Wang, Victor W. Day, and Kristin Bowman-James*

Department of Chemistry, University of Kansas, Lawrence, Kansas 66045, United States

Supporting Information

ABSTRACT: An amine/amide mixed covalent organic tetrahedral cage **1** (H_{12}) was synthesized and characterized. The H_{12} cage contains 12 amide NH groups plus four tertiary amine N groups, the latter of which are positioned in a pseudo-tetrahedral array. Crystallographic findings indicate that the tetrahedral host can adopt either a pseudo-C_3 symmetric "compressed tetrahedron" structure, or one in which there are two sets of three stacked pyridine units related by a pseudo-S_4 axis. The latter conformation is ideal for encapsulating small pentameric clusters, either a water molecule or a fluoride ion surrounded by a tetrahedral array of water molecules, i.e., $H_2O{\cdot}4H_2O$ or $F^-{\cdot}4H_2O$, as observed crystallographically. In solution, however, ^{19}F NMR spectroscopy indicates that H_{12} encapsulates fluoride ion through direct amide hydrogen bonding. By collectively combining one-dimensional ^1H, ^{13}C, and ^{19}F with two-dimensional $^1H-^1H$ COSY, $^1H-^{13}C$ HSQC, and $^1H-^{19}F$ HETCOR NMR techniques, the solution binding mode of fluoride can be ascertained as consisting of four sets of independent structural subunits with C_3 symmetry. A complex deuterium exchange process for the fluoride complex can also be unraveled by multiple NMR techniques.

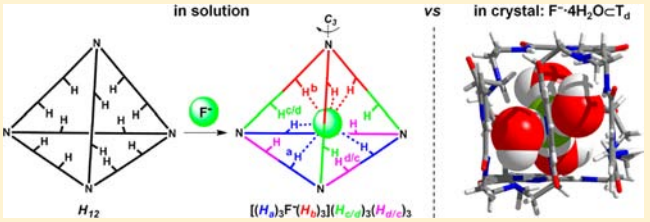

INTRODUCTION

Molecular capsules that can sequester molecules, ions, or a mixture of both, are popular supramolecular hosts because of the potential applications inherent in an isolated microenvironment.[1] For example, they can mimic the deep binding clefts in naturally occurring proteins in biological systems,[2] provide mini-reaction flasks for chemical transformations on the molecular scale,[3] or assist in the stabilization of highly reactive species.[4]

We recently communicated the crystal structure of a totally covalent organic tetrahedron host which possesses 12 potential amide hydrogen-bonding sites, **1** (H_{12}), Figure 1.[5] In one of its possible conformations, the tetrahedron is perfectly aligned for incorporation of a tetrahedral array of four water molecules.

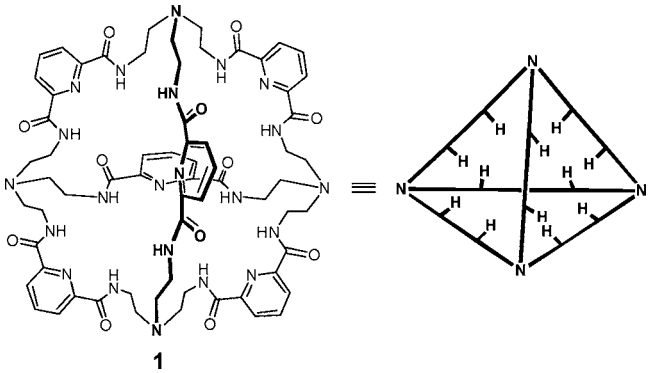

1

Figure 1. Structure of the tetrahedron, **1**.

Furthermore, a fifth small entity can be held in the water pocket, either another water molecule or a fluoride ion. The former "water" complex resembles one of the simplest possible water units made up of five water molecules and known as Walrafen's pentamer.[6] The latter "fluoride" complex resembles a caged solvated fluoride ion.

The supramolecular chemistry of fluoride ion is of particular interest, since fluoride possesses unique properties due to its high electronegativity and is also prevalent in biology and the environment.[7,8] Additionally, by virtue of its nuclear spin value of $+^1/_2$, fluoride is amenable to solution study by NMR. Hence, our interest in examining and comparing the solution and solid state structures of host–guest complexes led to our combined use of both X-ray crystallography and multinuclear and multidimensional NMR techniques to probe the supramolecular chemistry of the new tetrahedral host.

A number of tricyclic hosts providing tetrahedral cavities have been reported,[9−13] including several in the early years in supramolecular anion coordination.[10,11] While metal-directed self-assembly has more recently been a popular avenue to these cages,[9] organic tetrahedral cages linked entirely through covalent bonds remain rare.[10−13] The earliest example of a totally organic tetrahedron is the oxa aza tricyclic macrocycle known as the *soccer ball ligand* that was reported by Lehn and co-workers.[10] When tetraprotonated, this host can encapsulate chloride ion via hydrogen bonds with the four tetrahedrally positioned ammonium groups. When diprotonated, it is

Received: September 30, 2012
Published: November 29, 2012

   dx.doi.org/10.1021/ja3096762 | J. Am. Chem. Soc. 2013, 135, 392−399

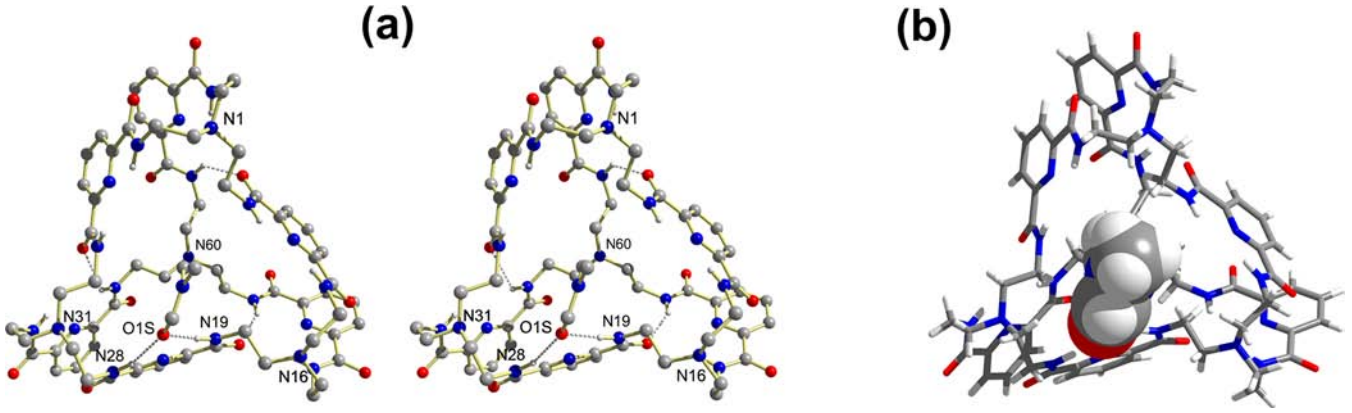

Figure 2. Views of the free base **1**, **A** down the C_3 axis. (a) Stereoview with the numbering scheme. (b) Corresponding perspective view with DMF shown in space-filling form. Solvent molecules outside the cavity are omitted for clarity. O, red; N, blue; C, gray; H, white.

thought to encapsulate a single molecule of water. The groups of Schmidtchen[11] and Ichikawa[12] have also provided insight to the roles of hydrogen bonding versus electrostatic interactions with their quaternized ammonium tetrahedrons. The larger dimensions of Schmidtchen's cavity allow for the selective incorporation of an iodide ion.[11]

Previously our group described the use of multinuclear ^{19}F and ^{1}H NMR techniques for elucidating the solution structure and chemistry of fluoride complexes with bicyclic polyammonium- and polyamide-based cryptands.[14,15] Here we use multiple NMR techniques, including both one-dimensional ^{1}H, ^{13}C, and ^{19}F and two-dimensional $^{1}H-^{1}H$ COSY, $^{1}H-^{13}C$ HSQC, and $^{1}H-^{19}F$ HETCOR, to describe the detailed solution structure of **1** in addition to crystallographic findings. Hence, not only does this study reveal the existence of secluded water clusters and fluoride solvation in a supramolecular host, but it also illustrates the important role that multinuclear and multidimensional NMR techniques can play in the elucidation of solution structure.

RESULTS AND DISCUSSION

Synthesis. Earlier, in the synthesis of bicyclic cryptand hosts for anions, our group used tris(2-aminoethyl)amines (tren) as bridgeheads and 2,6-diacetylpyridine units as linkers (bridgehead/linker ratio, 2:3).[15] This led to envisioning other possible connectivities using these building blocks. Two higher-order hosts were obtained using simple synthetic strategies. One is a cylindrical host consisting of two tetraamide-containing macrocycles linked by two diethylene diamidopyridine chains (bridgehead/linker ratio = 4:6).[16] The other host is the tetrahedral cage **1** (bridgehead/linker ratio also = 4:6).[5] Compared to the multiple steps needed to synthesize some of the tetrahedral cages reported previously,[10−12] only three simple steps were involved in this synthesis, as reported earlier.[5] The tetrahedron **1** was subsequently characterized by mass spectrometry (MS), NMR spectroscopy, and X-ray crystallography.

X-ray Crystallography. Crystallographic results indicated three different forms of the tetrahedron. These consisted of the free base with no encapsulated species, **A**, **1**·3DMF·$3H_2O$; a free base form with a different conformation and with five encapsulated water molecules, **B**, [H_2O·-$4H_2O$⊂**1**]·$10H_2O$·CH_3CN; and a third structure similar in conformation to **B**, but with an embedded fluoride ion surrounded (solvated) by four encapsulated molecules of water, **C**, [F^-·$4H_2O$⊂**1**]·Me_4N^+·$4H_2O$. Single crystals suitable for X-ray analysis were obtained by slow diffusion of ethyl acetate into a DMF solution of **1** for **A**, and slow evaporation of an acetonitrile solution of **1** in the presence of excess $Et_4N^+Cl^-$ and $Me_4N^+F^-$ for **B** and **C**, respectively.

As shown in Figure 2, in the "empty" host, **A**, the four bridgehead tertiary amine nitrogen atoms (N1, N16, N31, N60) and six diethylene diamidopyridine edges form a tetrahedron, with each face consisting of a hexaamido macrocycle. The bridgehead N---N distances consist of three longer separations, ranging from about 9.9 to 10.3, and three shorter distances, ranging from about 7.6 to 7.8 (Table 1). The three longer edges can be said to constitute the base of a pyramid, while the shorter edges are joined at what then becomes the apical nitrogen atom, N60, forming a pseudo-C_3 symmetric geometry. Three intramolecular interactions (two short, 2.933(5), 2.948(5) Å; one quite long, 3.236(6) Å) between the amido (N−H) and carbonyl (O═C) groups serve to lock conformation in place (Figure 2a). The resulting conformation is a compressed tetrahedron with a large open window at the base. A DMF molecule hovers right beneath the base, slightly intruding, with hydrogen bonds from its oxygen atom to N19 and N28 within one diamidopyridine cleft. The other two DMF and three water molecules reside in the crystal lattice between host molecules.

Table 1. Geometrical Parameters [Å] for the Tetrahedral Skeleton for Structure A, "Empty" 1; B, H_2O·$4H_2O$⊂1; and C, F^-·$4H_2O$⊂1

N---N	A	B	C
N1---N16	9.893	6.872	6.927
N1---N31	10.255	7.524	8.066
N1---N60	7.805	6.389	6.754
N16---N31	9.982	7.103	6.286
N16---N60	7.560	7.902	7.472
N31---N60	7.620	6.690	6.966

In **B**, **1** adopts a different conformation (Figure 3).[5] The bridgehead N---N distances range from 6.389 to 7.902 Å. These distances constitute a smaller range and are somewhat shorter on the average than those observed in **A** (Table 1). Two sets of three stacked diamidopyridine groups are almost orthogonal to each other and are related by a pseudo S_4 axis at opposite "sides" of the molecule. This conformation results in a cube-like box surrounding the guest contents as shown in Figure 3c. On

dx.doi.org/10.1021/ja3096762 | J. Am. Chem. Soc. 2013, 135, 392−399

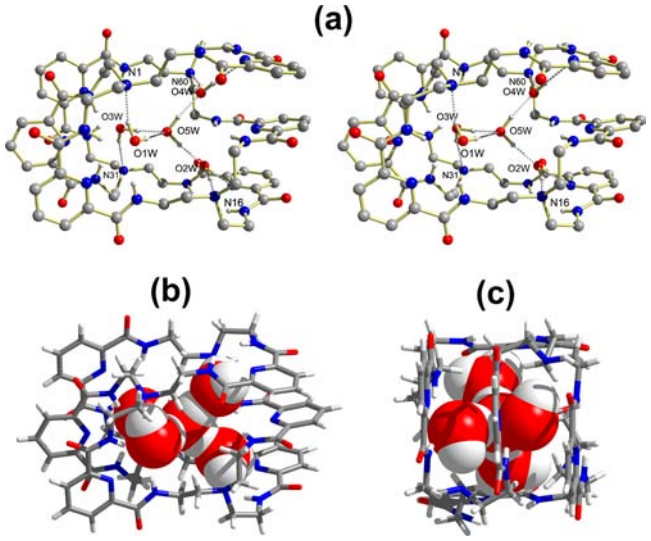

Figure 3. Views of $H_2O{\cdot}4H_2O{\subset}\mathbf{1}$, **B**. (a) Stereoview showing the numbering scheme. (b) Corresponding perspective view. (c) "Cube" view with the guests shown in space-filling forms in the latter two views. The solvent and water molecules outside the cavity are omitted for clarity. O, red; N, blue; C, gray; H, white.

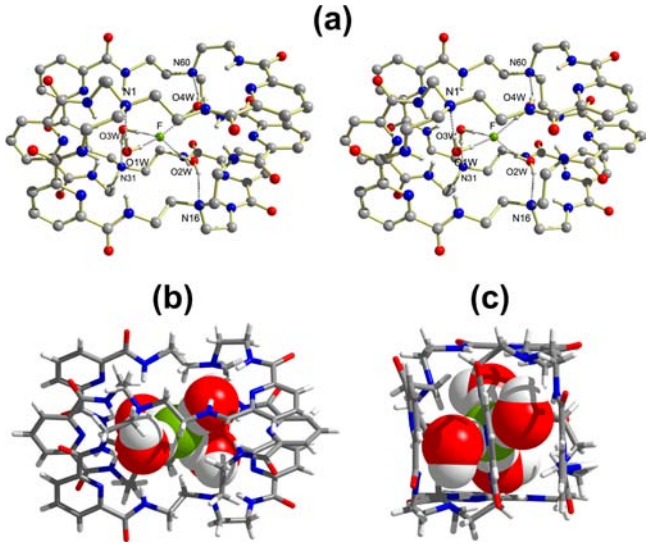

Figure 4. Views of $F^-{\cdot}4H_2O{\subset}\mathbf{1}$, **C**. (a) Stereoview showing the numbering scheme, (b) corresponding perspective view, and (c) "cube" view with the guests shown in space-filling forms in the latter two views. The Me_4N^+ ion and water molecules outside the cavity are omitted for clarity. O, red; F, green; N, blue; C, gray; H, white.

the front face of the cube, the three diamidopyridine edges form vertical "bars" holding the water cluster, and on the back, the other three edges form horizontal "bars." The multiple hydrogen-bonding sites within the host cavity (pyridine and bridgehead amine nitrogen atoms and amide NH groups) provide an almost tetrahedrally shaped hydrophilic cavity which is ideally suited for holding four encapsulated water molecules in a similar configuration. The bit of space available at the very center of the cavity is of sufficient size for a small fifth molecule or ion, which, in **B** is a molecule of water.

Such a tetrahedral array in a pentameric water cluster was first postulated in 1964 by Walrafen as one of the simplest hydrogen-bonded water networks.[6] On the basis of a careful search of the Cambridge Crystallographic Database for other sequestered tetrahedrally shaped, pentameric clusters, this may be the first crystallographic verification of an isolated Walrafen's pentamer enclosed within a supramolecular host capsule. The central water molecule, $H_2O(5w)$, is held solely by the four surrounding water molecules (O···O distances range from 2.649(2) to 2.751(3) Å). The tetrahedrally oriented bridgehead nitrogen atoms seem to play the major role of anchoring the other four water molecules (O···N distances range from 2.786(3) to 3.051(3) Å). Six of the amido groups and two pyridine nitrogen atoms act as additional hydrogen-bonding sites. See Table S2 in Supporting Information for a complete listing of hydrogen-bonding contacts.

In **C**, the host adopts a conformation similar to **B**. However, in this case the central atom is a fluoride ion, resulting in a discrete hydrated fluoride cluster, $F^-{\cdot}4H_2O$ (Figure 4, Table 1).[5] Although the two structures appear similar (Figures 3 and 4), in **C** all four water molecules are hydrogen-bond donors compared to only two in **B**. Such a difference in donor/acceptor properties is thought to play an important role in biological systems where a dynamic process known as hydrogen-bond switching occurs during binding and release of substrates and in enzymatic pathways.[17] Because of the availability of an extensive internal hydrogen-bonding network in **1**, the versatile host can readily adjust for the need for two additional hydrogen-bond donors by supplying two of its amide donor groups.

NMR of 1. In DMSO-d_6 at room temperature the ^1H and ^{13}C NMR spectra display only one set of simple signals representing the six equivalent diethylene-diamido-pyridine edges (Figure 5). The five observed resonances include one

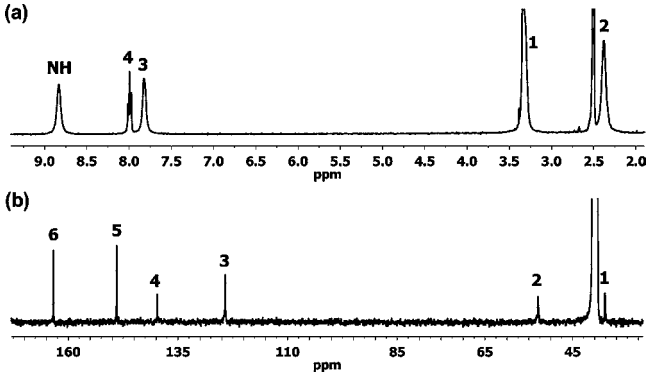

Figure 5. (a) ^1H and (b) ^{13}C NMR of the tetrahedral cage **1** (DMSO-d_6, 298 K). See Figure 7 for hydrogen and carbon assignments.

NH, and two CH_2 and pyridine signals anticipated as a result of either an averaged conformation or one optimal symmetrical conformation.

Variable-temperature ^1H NMR experiments (in DMF-d_7) indicated that the ^1H signals broadened as the temperature was gradually decreased to 238 K (Figure 6). As the temperature was further decreased to 208 K, a complicated set of sharp signals emerged, which probably indicates the existence of a single, dominant, nonsymmetrical rigid conformation. The original single N*H* signal shifted downfield and split into two main peaks, N*H*′ and N*H*″, confirmed by their disappearance upon D_2O exchange. At the same time, the pyridine and aliphatic signals became quite complex, shifting by various degrees either downfield or upfield. At 208 K, an unanticipated signal, which did not undergo deuterium exchange, appeared at

dx.doi.org/10.1021/ja3096762 | J. Am. Chem. Soc. 2013, 135, 392−399

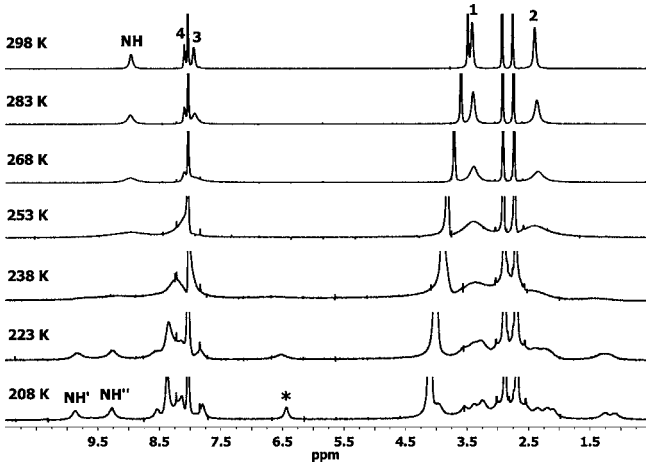

Figure 6. Variable temperature ^{1}H NMR (500 MHz) of the tetrahedral cage **1** in DMF-d_7. See Figure 7 for hydrogen assignments.

6.4 ppm (denoted by *). Since the possibility of its being an NH signal was ruled out, it could be one of the pyridine C*H* signals in the presence of significant shielding. If the low-temperature conformation were similar to the solid-state structure **B** or **C**, the central pyridine in each of the three stacked pyridine groups might experience such shielding effects.

NMR of 1·F$^-$. The 12 potential amide hydrogen-bond donors of **1** along with the numbering scheme are shown schematically in Figure 7. For clarity, the NMR spectra can be divided into two regions, the amide and pyridine region (Figure 8) and the aliphatic region (Figure 9).

During titration of **1** with *n*-Bu$_4$N$^+$F$^-$ in DMSO-d_6, the ^{1}H NMR spectra indicated a slow exchange process. When one equivalent of F$^-$ was added, the free host signals nearly disappeared completely, and a complicated set of new signals predominated. The spectrum did not change upon further

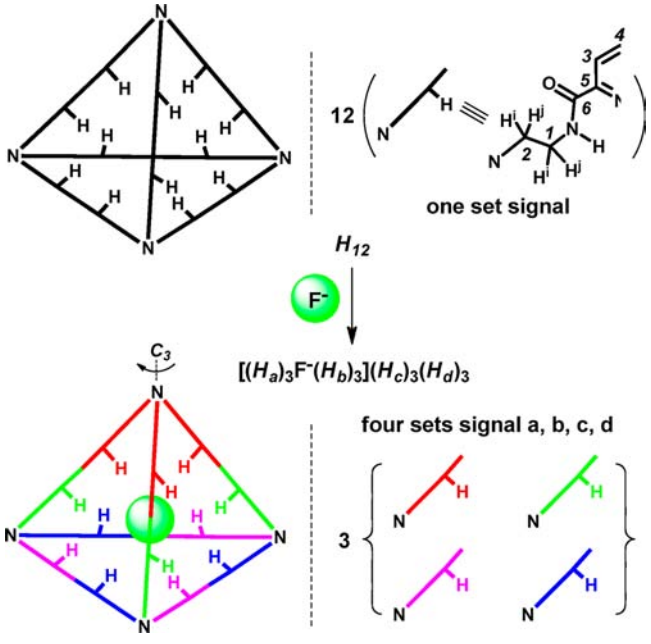

Figure 7. (Top) Scheme showing the T_d symmetry-equivalent amide NH bonds in **1**. (Bottom) Scheme showing breakdown of **1** to C_3 symmetry and four groups of three NH donors upon F$^-$encapsulation.

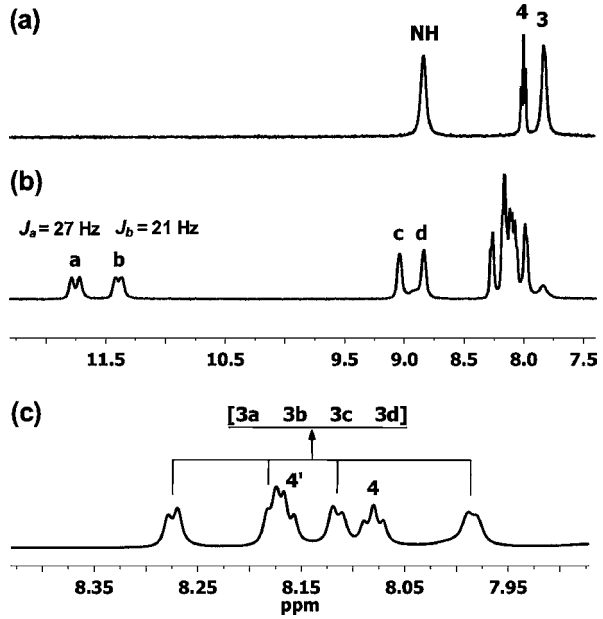

Figure 8. ^{1}H NMR (400 MHz, 298 K) of the amide and pyridine regions of (a) **1**, (b) **1** with one equivalent of *n*-Bu$_4$N$^+$F$^-$ (10 mM), and (c) ^{1}H NMR (800 MHz, 298 K) of the pyridine region of **1** with one equivalent of Me$_4$N$^+$F$^-$ (10 mM) in DMSO-d_6.

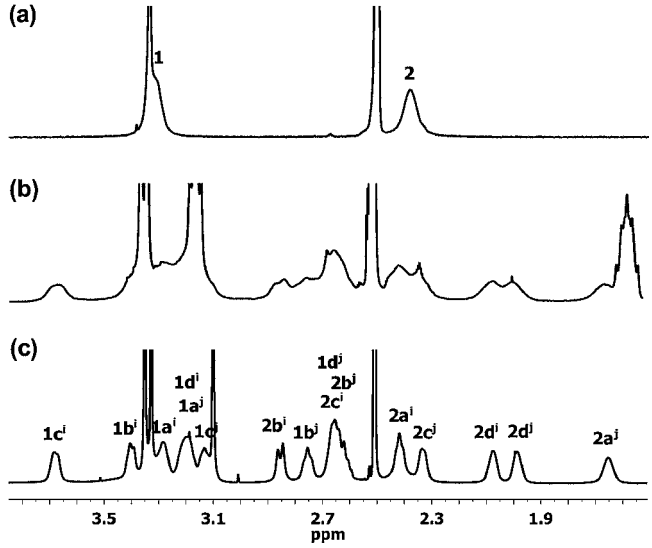

Figure 9. ^{1}H NMR (400 MHz, 298 K) of the aliphatic regions of (a) **1**, (b) **1** with one equivalent of (*n*-Bu)$_4$N$^+$F$^-$ (10 mM), and (c) ^{1}H NMR (800 MHz, 298 K) of **1** with one equivalent of Me$_4$N$^+$F$^-$ (10 mM) in DMSO-d_6.

addition of F$^-$ which indicated a strong 1:1 complex between **1** and F$^-$ ($K \approx 10^4$ M^{-1}).

Instead of the one amide signal in the free base (Figure 8a), four new amide NH signals appeared in the 1:1 complex (Figure 8b). Two doublets were significantly downfield shifted (H_a, H_b, δ = 11.78, 11.42 ppm), indicating strong coupling with the $I = {}^1/_2$F$^-$ nucleus ($^{H-F}J_a$ = 27 Hz, $^{H-F}J_b$ = 21 Hz). Two additional singlets (H_c, H_d, δ = 9.05, 8.84 ppm), also appeared, not shifted much from the original amide signal at 8.83 ppm, indicating only weak interaction at most (Table 2). These two signals are reminiscent of the low-temperature NMR of the free base (Figure 6), where the amide resonance split into two signals at 9.86 and 9.27 ppm. However, unlike in the free base

dx.doi.org/10.1021/ja3096762 | J. Am. Chem. Soc. 2013, 135, 392−399

Table 2. Partial ^{1}H and ^{13}C NMR Chemical Shift (δ) of the Tetrahedral Cage 1 and the Complex 1·F$^-$, Cryptand 2, and the Complex 2·F$^-$[a]

		^{1}H					^{13}C	
δ (ppm)		NH	CH_2^1 (*i*, *j*)		CH_2^2 (*i*, *j*)		C ^{1}	C ^{2}
1		8.83	3.31		2.38		37.6	52.9
2		8.86	3.38		3.00		37.9	53.8
1·F$^-$	a	11.78	3.28	3.20	2.42	1.65	40.3	49.8
	b	11.42	3.40	2.75	2.85	2.62	41.0	62.7
	c	9.05	3.68	3.13	2.65	2.34	35.9	52.9
	d	8.84	3.20	2.65	2.08	1.99	36.3	52.9
2·F$^-$		11.85	3.30	2.61	2.80	2.61	40.9	62.5

[a]See Figure 7 for signal assignments and Figure 11 for the structure of the cryptand.

at low temperatures, there is no new signal at 6.5 ppm in the F$^-$ complex.

The ethylene group signals (NHCH_2^1CH_2^2) also split into four sets of independent signals (Figure 9b and c). Additionally, the two protons on the same methylene group became nonequivalent (denoted as H^i and H^j). As a result, eight signals (4 methylene groups × 2 independent hydrogen atoms on each) exist for each of the two kinds of methylene groups (Figure 9, Table 2). With the exception of overlap of only a few signals, the entire set of 16 signals for the symmetry-independent methylene hydrogen atoms can be obtained in the high-resolution 800 MHz NMR spectrum (Figure 9c). $Me_4N^+F^-$ was used as the anion source for this spectrum to avoid the interference of the multiple signals of *n*-Bu_4N^+. Moreover, all of these signals have equal integrations (3H). $^{1}H-^{1}H$ COSY NMR and $^{1}H-^{13}C$ HSQC NMR both provided confirming evidence for the four independent sets of ethylene signals (Figures S2–S4 in Supporting Information).

H_a and H_b were confirmed as the proton sets associated with the F$^-$ through hydrogen bonding by $^{1}H-^{19}F$ HETCOR NMR. Protic DMSO was used for the ^{19}F studies to circumvent complications from deuterium exchange. The 1:1 complex of F$^-$ with **1** reveals a septet at −119.5 ppm ($^{H-F}J_{ave}$ = 24 Hz) as shown at the top of the HETCOR NMR in Figure 10.[5] A single septet instead of a higher order multiplet occurs since the two NH protons, H_a and H_b, have similar chemical shifts and display approximate magnetic equivalence toward F$^-$. The pattern then follows a simplified $2nI$ + 1, with an averaged coupling constant. $^{1}H-^{19}F$ HETCOR NMR revealed two correlated cross peaks, with the stronger coupling with H_a showing the higher correlated signal intensity (Figure 10). This finding provides added evidence for the viability of the formula $[(H_a)_3F^-(H_b)_3](H_c)_3(H_d)_3$, where both H_a and H_b are hydrogen bonded with an internal fluoride ion.

In summary, solution NMR for the fluoride complex indicated a reduction of the apparent symmetry from T_d to C_3. Four distinct $NHCH_2CH_2$ units have been identified, each comprising one-half of an edge of the tetrahedron. Two of the units are associated with the sides of the pyramid (red and green in Figure 7) and two comprise the base (pink and blue in Figure 7). Furthermore, each of the amide signals has been correlated with a specific CH_2CH_2 unit. In order for the symmetry to prevail, the encapsulated F$^-$ must sit on the C_3 axis. What is clearly evident, however, is that the solution structure does not correlate with the solvated fluoride structure seen in the solid state.

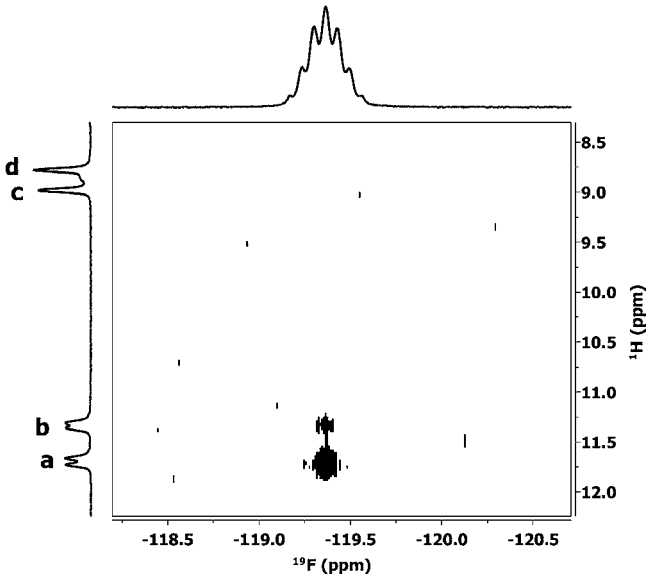

Figure 10. $^{1}H-^{19}F$ HETCOR NMR (400 MHz, 298 K) of **1** with one equivalent of (*n*-Bu)$_4N^+F^-$ (10 mM) in protic DMSO.

Pinpointing the F$^-$ Position using Cryptand Data. Comparison of the solution fluoride NMR with **1** with previous findings for an amide-based cryptand enabled additional insight into the solution structure. In previous reports, we demonstrated solution encapsulation of F$^-$ in an amide-based cryptand with pyridine spacers, **2**, (Figure 11) using ^{19}F NMR spectroscopy.[15] In **2**·F$^-$ six chemically equivalent amide NH groups were found to hydrogen bond with the fluoride ion, consistent with the solid-state structure and manifested by a single set of signals for the NH, CH_2^1, and CH_2^2 protons (Table 2).

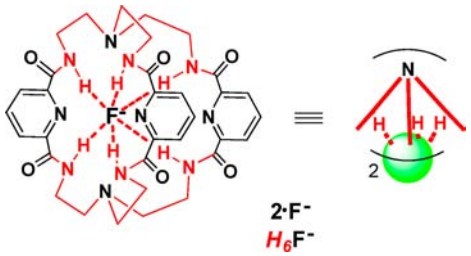

Figure 11. Structure of the amide-based cryptand, **2**, with F$^-$.

A structural similarity exists for the three trigonally situated NH protons (in red) at the apex of **1** (Figure 7) and the bridgehead-associated amide protons (also in red) in **2** (Figure 11). Furthermore, the chemical shifts for the amide NH group of the H_a and H_b protons (the ones assumed to be hydrogen bonded with the fluoride) in **1** more closely resemble that of **2** compared to groups H_c and H_d protons (Table 2). Furthermore, in examining the CH_2 chemical shifts, the best correlation with **2** is seen with the H_b protons of **1**. This becomes especially apparent for the very similar ^{13}C chemical shifts for C^2 (62.7 ppm for group H_b in **1** and 62.5 ppm for **2**). Hence the H_b set of NH protons that are hydrogen bonded with **1** can most probably be assigned to the three symmetry-equivalent NH groups at the apex of the tetrahedron.

The general position of the second set of three NH protons, NH_a can be deduced from a symmetry argument. If it were the

dx.doi.org/10.1021/ja3096762 | J. Am. Chem. Soc. 2013, 135, 392–399

remaining set of amides (green) adjoining the three amides at the top of the tetrahedron, the two subunits forming the base of the pyramid (pink and blue) should be symmetry equivalent. In this case only three symmetry-independent amide signals would appear in the spectrum, with a 1:1:2 integration (3H:3H:6H). However, that is not the case; thus, the other set of protons hydrogen bonded to the F^- ion (H_a) must be one of the two sets of subunits (pink or blue) making up the base of the tetrahedron (Figure 7).

Thus F^- interacts most closely with one of the two symmetry-independent sets of hydrogen atoms of the base triangle (either pink or blue) of the compressed pyramid, H_a. The other three hydrogen-bonded protons comprise the three amide hydrogen atoms at the apex of the pyramid, H_b.

Deuterium Exchange Chemistry. While the protic DMSO spectrum was simple as noted earlier, in DMSO-d_6 a complex deuterium exchange process was manifested (Figure 12a and b, respectively), reminiscent of that seen for the fluoride cryptand complex of **2**.[15] The initial exchange process was rapid, and no further change was noted with time or heating. The pattern consists of an initial septet, with a sequence of rather broad multiplets of decreasing multiplicity progressively upfield.

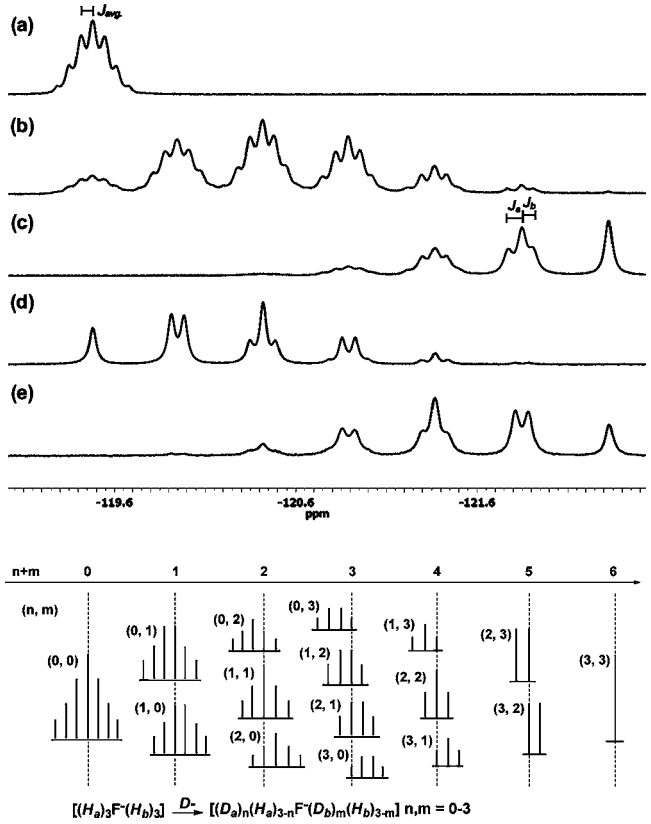

Figure 12. Top series of spectra: ^{19}F NMR (400 MHz, 298 K) of **1** with one equivalent of $(n\text{-Bu})_4N^+F^-$ (10 mM). (a) **1**, protic DMSO, (b) **1**, DMSO-d_6, (c) **1**-d_{12}, DMSO-d_6, (d) **1**, DMSO-d_6, with ^1H inverse-gated broad-band decoupling, (e) **1**-d_{12}, DMSO-d_6, with ^1H inverse-gated broad-band decoupling. Bottom: multiplet deconvoluted according to the formula $[(D_a)_n(H_a)_{3-n}F^-(D_b)_m(H_b)_{3-m}]$ where n, m = 0−3.

In the hexaamido cryptand **2**, an initial septet (due to coupling of the fluoride with six equivalent amide hydrogen atoms), was joined with time by the appearance of a sequence of multiplets from sextet down to singlet. This pattern was identified as indicative of exchange of one, two, three, etc. up to all six NH hydrogen atoms with deuterium. In the case of **1**, however, the resulting spectra appeared to be the result of a more complex solution chemistry, since the multiplets were somewhat broad and did not have the symmetry anticipated for a simple equivalent exchange process.

To understand this chemistry better, the deuterated free host **1**-d_{12} (***D*****$_{12}$**) was prepared by deuterium exchange of **1** with CD_3OD/D_2O. The resulting spectrum gave a series of multiplets starting from the fully deuterated singlet signal at −122.3 ppm (Figure 12c). By overlapping the two spectra (Figure 12b and c), the series was determined as being comprised of seven multiplets, indicative of sequential deuterium replacement of six protons. However, unlike the smooth multiplet sequence observed in **2**, this series did not appear to be the simple sequential replacement of 1 through 6 hydrogen atoms. For example, the multiplet next to the singlet in Figure 12c was not the anticipated doublet, but rather an unsymmetrical triplet, and the one next to that was a broad quintet rather than a triplet.

Unlike **2**, with six equivalent amide hydrogen atoms, **1** possesses four independent sets of hydrogen atoms (H_a, H_b, H_c, and H_d), each consisting of three hydrogen atoms. However, only two sets, H_a and H_b, are strongly hydrogen bonded with F^- in solution. Therefore, while random deuterium exchange is occurring for all the amide NH protons, $^1H-^{19}F$ coupling is only observed for the six NH protons that are hydrogen bonded with F^- ion. The interval between each adjacent multiplet ($\Delta\delta$) equals −0.47 ppm, which is quite similar to what is observed in the cryptand complex, **2**·F^- (Figure 11), where $\Delta\delta$ = −0.46 ppm.[15] In both complexes, **1**·F^- and **2**·F^-, the initial multiplet is a septet, and the last signal is a singlet, the latter corresponding to complete deuterium exchange of the associated six amide protons.

Because of the two independent hydrogen-bonded groups, H_a and H_b, in **1**·F^-, deuterium exchange involving the hydrogen-bonded amides can occur on either H_a or H_b, which would be anticipated to display slightly different F^- chemical shifts. This is the cause of the more complex multiplet series seen for **1**·F^-. Hence, as seen in the diagram below the spectra in Figure 12, the second multiplet, $n + m = 1$ at −119.9 ppm, consists of two overlapping sextets corresponding to $[(D_a)_0(H_a)_3F^-(D_b)_1(H_b)_2]$ (n = 0 and m = 1) and $[(D_a)_1(H_a)_2F^-(D_b)_0(H_b)_3]$ (n = 1 and m = 0) with slightly different chemical shifts ($\Delta\delta$ = −0.068 ppm). The minor chemical shift difference between the two deuterated species is equal to 27 Hz, which very nearly equals the coupling constant (J_{ave} = 24 Hz). This coincidence makes the two sextets overlap like an apparent septet. At the other end of the spectrum, the sixth multiplet at −121.9 ppm, corresponding to $n + m = 5$, looks like a triplet but is actually two doublets that correspond to the molecular formula $[(D_a)_2(H_a)_1F^-(D_b)_3(H_b)_0]$, where n = 2 and m = 3 and $[(D_a)_3(H_a)_0F^-(D_b)_2(H_b)_1]$, where n = 3 and m = 2. A similar analysis can be performed for the other multiplets.

^1H inverse-gated broad-band decoupling of the ^{19}F NMR spectra (Figure 12d and e), where all of the couplings between ^{19}F and ^1H nucleus were eliminated, supported these conclusions. In these two spectra, one starting with non-deuterated **1**, the other with totally deuterated **1**, the seven multiplets are simplified, and each individual signal in the multiplet represents one specific deuterated species. For

dx.doi.org/10.1021/ja3096762 | J. Am. Chem. Soc. 2013, 135, 392−399

example, a single resonance signal is observed for the first (Figure 12d) and the last multiplets (Figure 12e), corresponding to just one possibility for each, either no deuterium exchange, where $n = m = 0$ or complete exchange, where $n = m = 3$, respectively. Two signals (a doublet) are seen for the second and sixth multiplets (Figure 12d and e, respectively), corresponding to the two possibilities for each, either $n = 0$ and $m = 1$ or $n = 1$ and $m = 0$ for the second multiplet, and either $n = 2$, $m = 3$ or $n = 3$, $m = 2$ for the sixth. The intensities of the two signals in each the multiplets are approximately equal, indicating an equal probability for the two deuterium exchange possibilities.

CONCLUSIONS

The three crystal structures serve to highlight the conformational flexibility of **1** along with its variety of handily placed hydrogen-bonding sites. In the years after Walrafen's predication of the tetrahedrally shaped pentameric water cluster, a number of researchers have explored physical (primarily IR and Raman)[6,18] and theoretical[19] evidence of its existence both in solution and the solid state. In **B**, the identification of a crystalline, isolated cluster of Walrafen's pentamer serves as further confirmation of the existence of this form of water. In **C**, the characterization of an isolated solvated fluoride ion serves to add to information about the solvation properties of this ion and also provides a snapshot of hydrogen-bond switching when compared with the homomolecular water cluster in **B**. While **A** is apparently the outlier in the series in terms of solid-state conformation, it may indeed be a prevalent structural contender for the solution structure of the F^- complex. Its compressed pyramidal structure would result in nonequivalent NH signals and would be a likely distortion to occur for the hydrogen-bonding mode determined by the solution NMR studies of the fluoride complex.

The solution structure of the fluoride complex with **1** is clearly independent of the solid-state water-solvated structure. Upon binding fluoride ion in DMSO, the T_d-like symmetry is lowered to an apparent C_3 symmetry, with four sets of independent subunits, $[(H_a)_3F^-(H_b)_3](H_c)_3(H_d)_3$, possibly similar to the structure of the free base **A**. The fluoride sits on the C_3 axis and associates with two symmetry-different sets, totaling six amide protons, (H_a) three (H_b) from the apical tren unit and the other three from the bottom face.

The use of multiple NMR probes also allowed for a complex deuterium exchange process to be unraveled in the fluoride complex. While only the exchange of the NH protons that were hydrogen bonded with the fluoride ion could be observed in the ^{19}F NMR, these capabilities point to the power of the tool for other, similar host–guest interactions. Thus, taken in tandem, X-ray crystallography and the current arsenal of NMR techniques can open the door to a better understanding of the structural similarities and differences in solid state and solution in host–guest chemistry. Ultimately, this understanding can pave the way for the design of more selective and innovative supramolecular hosts.

ASSOCIATED CONTENT

Supporting Information

Crystallographic data in CIF format. Lists of hydrogen-bonding contacts in the structures **B** and **C**. NMR experimental procedure and additional ^1H, ^{13}C, $^1H-^1H$ COSY, $^1H-^{13}C$ HSQC NMR spectra. This material is available free of charge via the Internet at http://pubs.acs.org.

AUTHOR INFORMATION

Corresponding Author

kbjames@ku.edu

Notes

The authors declare no competing financial interest.

ACKNOWLEDGMENTS

We thank the National Science Foundation for support of this work (CHE-0854967) and for purchase of the X-ray diffractometer (CHE-0923449). We also thank Dr. J. T. Douglas for NMR technical assistance and helpful discussion.

REFERENCES

(1) (a) Cram, D. J. *Nature* **1992**, *356*, 29–36. (b) MacGillivray, L. R.; Atwood, J. L. *Angew. Chem., Int. Ed.* **1999**, *38*, 1018–1033. (c) Hof, F.; Craig, S. L.; Nuckolls, C.; Rebek, J., Jr. *Angew. Chem., Int. Ed.* **2002**, *41*, 1488–1508. (d) Vriezema, D. M.; Aragonès, M. C.; Elemans, J. A. A. W.; Cornelissen, J. J. L. M.; Rowan, A. E.; Nolte, R. J. M. *Chem. Rev.* **2005**, *105*, 1445–1489.

(2) (a) Breslow, R.; Dong, S. D. *Chem. Rev.* **1998**, *98*, 1997–2011. (b) Hof, F.; Trembleau, L.; Ullrich, E. C.; Rebek, J., Jr. *Angew. Chem., Int. Ed.* **2003**, *42*, 3150–3153. (c) Butterfield, S. M.; Rebek, J., Jr. *J. Am. Chem. Soc.* **2006**, *128*, 15366–15367. (d) Hooley, R. J.; Rebek, J., Jr. *Chem. Biol.* **2009**, *16*, 255–264.

(3) (a) Fiedler, D.; Leung, D. H.; Bergman, R. G.; Raymond, K. N. *Acc. Chem. Res.* **2005**, *38*, 351–360. (b) Iwasawa, T.; Hooley, R. J.; Rebek, J., Jr. *Science* **2007**, *317*, 493–496. (c) Pluth, M. D.; Bergman, R. G.; Raymond, K. N. *Acc. Chem. Res.* **2009**, *42*, 1650–1659. (d) Yoshizawa, M.; Klosterman, J. K.; Fujita, M. *Angew. Chem., Int. Ed.* **2009**, *48*, 3418–3438.

(4) (a) Cram, D. J.; Tanner, M. E.; Thomas, R. *Angew. Chem., Int. Ed. Engl.* **1991**, *30*, 1024–1027. (b) Warmuth, R. *Angew. Chem., Int. Ed. Engl.* **1997**, *36*, 1347–1350. (c) Yoshizawa, M.; Kusukawa, T.; Fujita, M.; Yamaguchi, K. *J. Am. Chem. Soc.* **2000**, *122*, 6311–6312. (d) Mal, P.; Breiner, B.; Rissanen, K.; Nitschke, J. R. *Science* **2009**, *324*, 1697–1699.

(5) Wang, Q.-Q.; Day, V. W.; Bowman-James, K. *Angew. Chem., Int. Ed.* **2012**, *51*, 2119–2123.

(6) (a) Walrafen, G. E. *J. Chem. Phys.* **1964**, *40*, 3249–3256. (b) Walrafen, G. E. *J. Chem. Phys.* **1967**, *47*, 114–126. (c) Monosmith, W. B.; Walrafen, G. E. *J. Chem. Phys.* **1984**, *81*, 669–674. (d) Walrafen, G. E.; Hokmabadi, M. S.; Yang, W.-H. *J. Chem. Phys.* **1986**, *85*, 6964–6969. (e) Walrafen, G. E.; Fisher, M. R.; Hokmabadi, M. S.; Yang, W.-H. *J. Chem. Phys.* **1986**, *85*, 6970–6982. (f) Walrafen, G. E.; Yang, W.-H.; Chu, Y. C.; Hokmabadi, M. S. *J. Phys. Chem.* **1996**, *100*, 1381–1391.

(7) (a) Cametti, M.; Rissanen, K. *Chem. Commun.* **2009**, 2809–2829. (b) Wade, C. R.; Broomsgrove, A. E. J.; Aldridge, S.; Gabbaï, F. P. *Chem. Rev.* **2010**, *110*, 3958–3984.

(8) (a) Colquhoun, J. *Perspect. Biol. Med.* **1997**, *41*, 1–16. (b) Diesendorf, M.; Colquhoun, J.; Spittle, B. J.; Everingham, D. N.; Clutterbuck, F. W. *Aust. N. Z. J. Public Health* **1997**, *21*, 187–190. (c) Carton, R. J. *Fluoride* **2006**, *39*, 163–172.

(9) (a) Mann, S.; Huttner, G.; Zsolnai, L.; Heinze, K. *Angew. Chem., Int. Ed. Engl.* **1996**, *35*, 2808–2809. (b) Fleming, J. S.; Mann, K. L. V.; Carraz, C. A.; Psillakis, E.; Jeffery, J. C.; McCleverty, J. A.; Ward, M. D. *Angew. Chem., Int. Ed.* **1998**, *37*, 1279–1281. (c) Caulder, D. L.; Raymond, K. N. *Acc. Chem. Res.* **1999**, *32*, 975–982. (d) Albrecht, M.; Ingo, J. A.; Fröhlich, R. *Chem. Commun.* **2005**, 157–165. (e) Mal, P.; Schultz, D.; Beyeh, K.; Rissanen, K.; Nitschke, J. R. *Angew. Chem., Int. Ed.* **2008**, *47*, 8297–8301. (f) Saalfrank, R. W.; Maid, H.; Scheurer, A. *Angew. Chem., Int. Ed.* **2008**, *47*, 8794–8824. (g) Glasson, C. R. K.; Meehan, G. V.; Clegg, J. K.; Lindoy, L. F.; Turner, P.; Duriska, M. B.; Willis, R. *Chem. Commun.* **2008**, 1190–1192. (h) Custelcean, R.; Bosano, J.; Bonnesen, P. V.; Kertesz, V.; Hay, B. P. *Angew. Chem., Int. Ed.* **2009**, *48*, 4025–4029. (i) Hristova, Y. R.; Smulders, M. M. J.; Clegg, J. K.; Breiner, B.; Nitschke, J. R. *Chem. Sci.* **2011**, *2*, 638–641.

(j) Clegg, J. K.; Li, F.; Jolliffe, K. A.; Meehan, G. V.; Lindoy, L. F. *Chem. Commun.* **2011**, *47*, 6042−6044. (k) Chakrabarty, R.; Mukherjee, P. S.; Stang, P. J. *Chem. Rev.* **2011**, *111*, 6810−6918. (l) Bilbeisi, R. A.; Clegg, J. K.; Elgrishi, N.; de Hatten, X.; Devillard, M.; Breiner, B.; Mal, P.; Nitschke, J. R. *J. Am. Chem. Soc.* **2012**, *134*, 5110−5119.

(10) (a) Graf, E.; Lehn, J.-M. *J. Am. Chem. Soc.* **1975**, *97*, 5022−5024. (b) Graf, E.; Lehn, J.-M. *J. Am. Chem. Soc.* **1976**, *98*, 6403−6405. (c) Metz, B.; Rosalky, J. M.; Weiss, R. *J. Chem. Soc., Chem. Commun.* **1976**, 533−534. (d) Graf, E.; Lehn, J.-M. *Helv. Chim. Acta* **1981**, *64*, 1040−1057. (e) Lehn, J.-M. *Pure Appl. Chem.* **1977**, *49*, 857−870.

(11) (a) Schmidtchen, F. P. *Angew. Chem., Int. Ed. Engl.* **1977**, *16*, 720−721. (b) Schmidtchen, F. P.; Müller, G. *J. Chem. Soc., Chem. Commun.* **1984**, 1115−1116. (c) Worm, K.; Schmidtchen, F. P.; Schier, A.; Schäfer, A.; Hesse, M. *Angew. Chem., Int. Ed. Engl.* **1994**, *33*, 327−329. (d) Schmidtchen, F. P.; Berger, M. *Chem. Rev.* **1997**, *97*, 1609−1646.

(12) (a) Ichikawa, K.; Yamamoto, A.; Hossain, M. A. *Chem. Lett.* **1993**, 2175−2178. (b) Hossain, M. A.; Ichikawa, K. *Tetrahedron Lett.* **1994**, *35*, 8393−8396. (c) Ichikawa, K.; Hossain, M. A.; Tamura, T.; Kamo, N. *Supramol. Chem.* **1995**, *5*, 219−224. (d) Hossain, M. A.; Ichikawa, K. *Chem. Lett.* **1996**, 553−554. (e) Ichikawa, K.; Hossain, M. A. *Chem. Commun.* **1996**, 1721−1722.

(13) (a) Takemura, H.; Shinmyozu, T.; Inazu, T. *J. Am. Chem. Soc.* **1991**, *113*, 1323−1331. (b) Mastalerz, M. *Chem. Commun.* **2008**, 4756−4758. (c) Skowronek, P.; Gawronski, J. *Org. Lett.* **2008**, *10*, 4755−4758. (d) Tozawa, T.; Jones, J. T. A.; Swamy, S. I.; Jiang, S.; Adams, D. J.; Shakespeare, S.; Clowes, R.; Bradshaw, D.; Hasell, T.; Chong, S. Y.; Tang, C.; Thompson, S.; Parker, J.; Trewin, A.; Bacsa, J.; Slawin, A. M. Z.; Steiner, A.; Cooper, A. I. *Nat. Mater.* **2009**, *8*, 973−978. (e) Hasell, T.; Wu, X.; Jones, J. T. A.; Bacsa, J.; Steiner, A.; Mitra, T.; Trewin, A.; Adams, D. J.; Cooper, A. I. *Nat. Chem.* **2010**, *2*, 750−755. (f) Swamy, S. I.; Bacsa, J.; Jones, J. T. A.; Stylianou, K. C.; Steiner, A.; Ritchie, L. K.; Hasell, T.; Gould, J. A.; Laybourn, A.; Khimyak, Y. Z.; Adams, D. J.; Rosseinsky, M. J.; Cooper, A. I. *J. Am. Chem. Soc.* **2010**, *132*, 12773−14775.

(14) Mason, S.; Llinares, J. M.; Morton, M.; Clifford, T.; Bowman-James, K. *J. Am. Chem. Soc.* **2000**, *122*, 1814−1815.

(15) (a) Kang, S. O.; Llinares, J. M.; Powell, D.; VanderVelde, D.; Bowman-James, K. *J. Am. Chem. Soc.* **2003**, *125*, 10152−10153. (b) Kang, S. O.; VanderVelde, D.; Powell, D.; Bowman-James, K. *J. Am. Chem. Soc.* **2004**, *126*, 12272−12273. (c) Kang, S. O.; Day, V. W.; Bowman-James, K. *J. Org. Chem.* **2010**, *75*, 277−283.

(16) Wang, Q.-Q.; Day, V. W.; Bowman-James, K. *Chem. Sci.* **2011**, *2*, 1735−1738.

(17) (a) Kropman, M. F.; Bakker, H. J. *Science* **2001**, *291*, 2118−2120. (b) Modig, K.; Liepinsh, E.; Otting, G.; Halle, B. *J. Am. Chem. Soc.* **2004**, *126*, 102−114. (c) Park, S.; Fayer, M. D. *Proc. Natl. Acad. Sci. U.S.A.* **2007**, *104*, 16731−16738. (d) Moilanen, D. E.; Wong, D.; Rosenfeld, D. E.; Fenn, E. E.; Fayer, M. D. *Proc. Natl. Acad. Sci. U.S.A.* **2009**, *106*, 375−380.

(18) Liu, K.; Brown, M. G.; Cruzan, J. D.; Saykally, R. J. *Science* **1996**, *271*, 62−64.

(19) (a) Wales, D. J.; Walsh, T. R. *J. Chem. Phys.* **1996**, *105*, 6957−6971. (b) Balasubramanian, K. *J. Phys. Chem. A* **2004**, *108*, 5527−5536. (c) Day, M. B.; Kirschner, K. N.; Shields, G. C. *J. Phys. Chem. A* **2005**, *109*, 6773−6778.